ULF wave radial diffusion in the radiation belts as determined through a multi-parameter study

S. Dimitrakoudis[(1)], I.R. Mann[(3)], G. Balasis[(1)], C. Papadimitriou[(1,2)], A. Anastasiadis[(1)], and I.A. Daglis[(2,1)]

(1) National Observatory of Athens, Athens, Greece

(2) National & Kapodistrian University of Athens, Athens, Greece

(3) University of Alberta, Alberta, Canada

HELAS, Thessaloniki, 29/6/2015

Outline

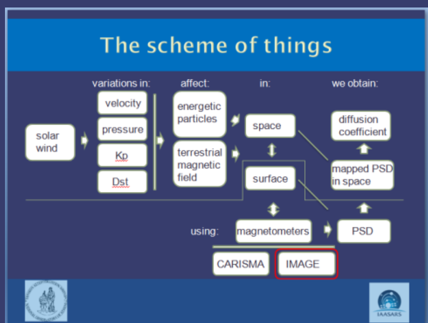

I) Introduction

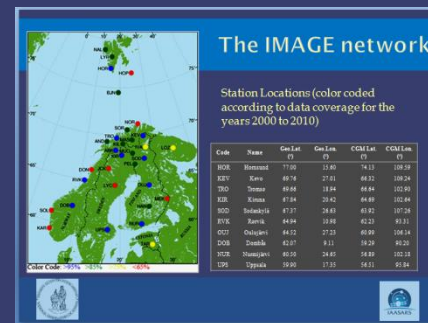

II) Observations

III) Calculations & Results

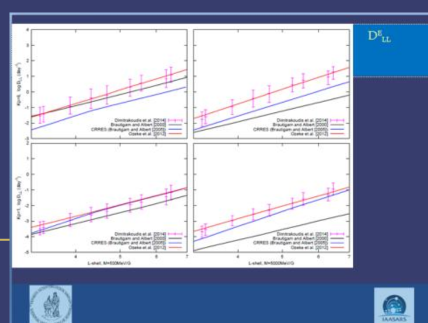

IV) Summary

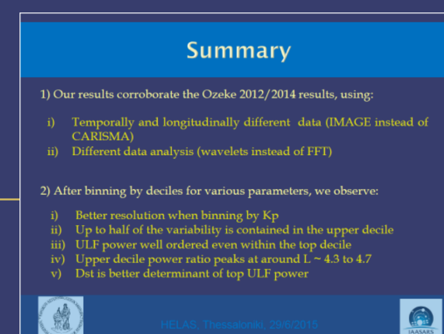

Inner and outer radiation belts

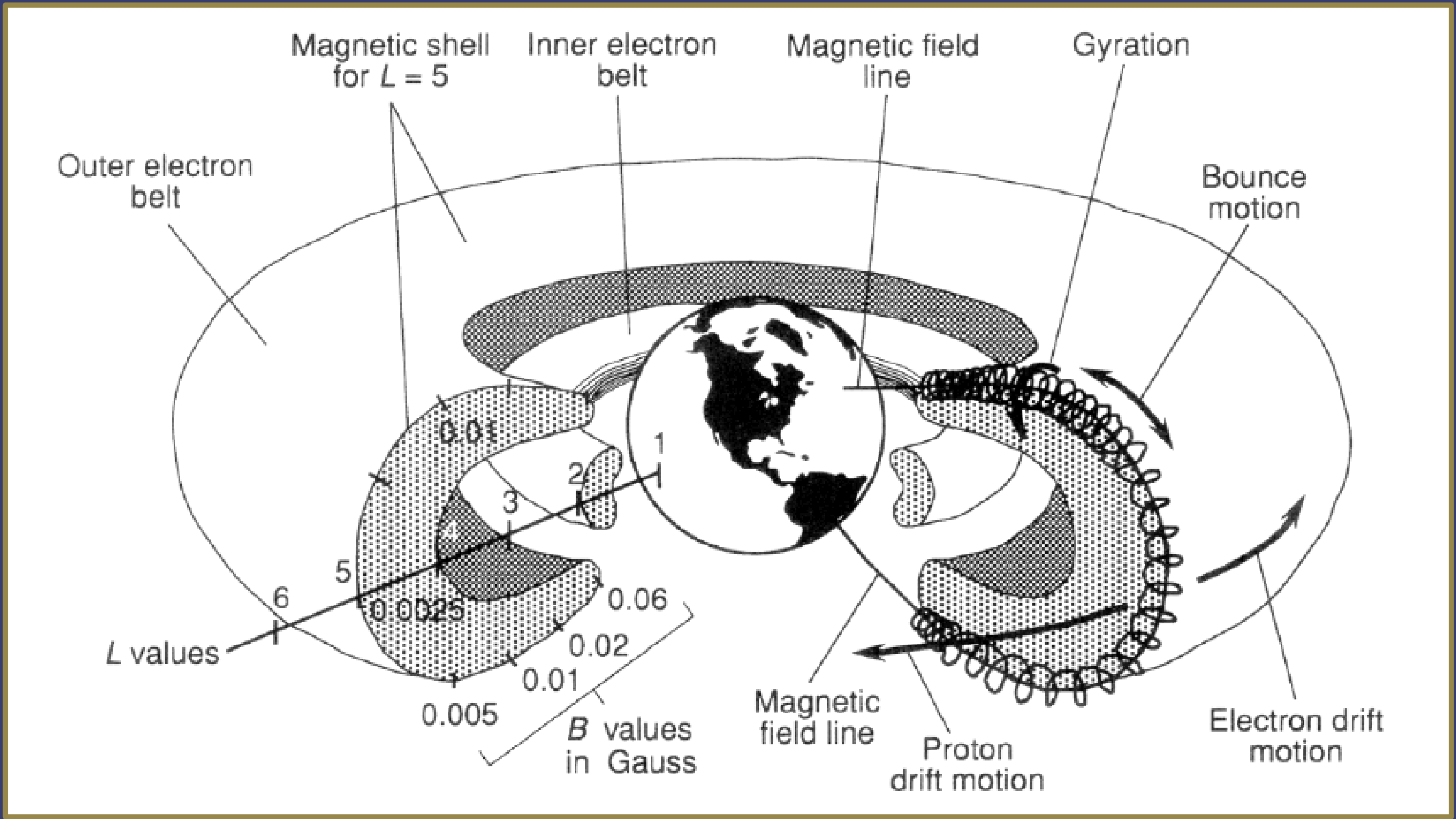

Mitchell 1994

Proton energies: 100keV – 200MeV

Electron energies: 100keV – 15MeV

ULF
wave
generation

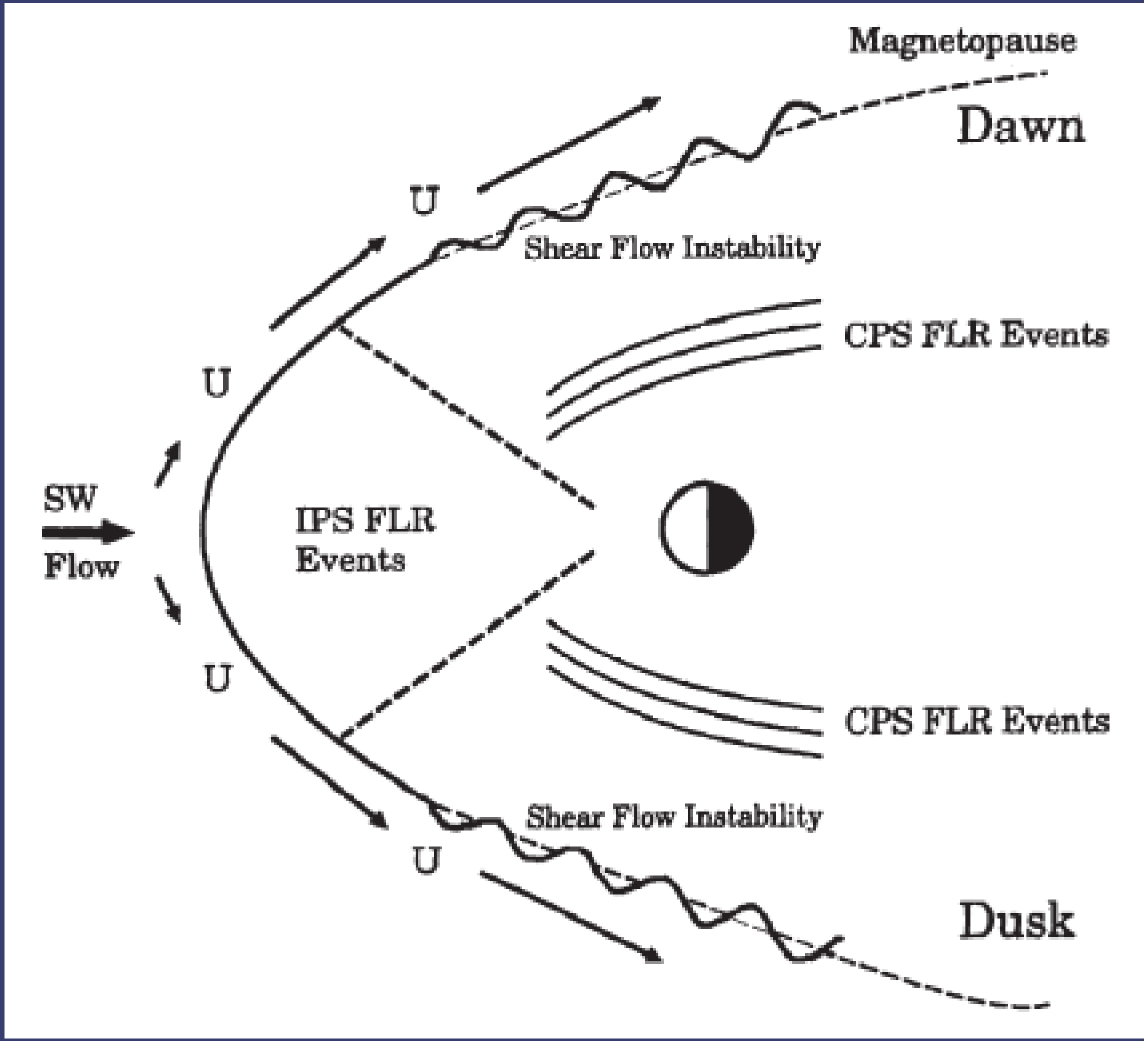

Mathie & Mann 2000

The scheme of things

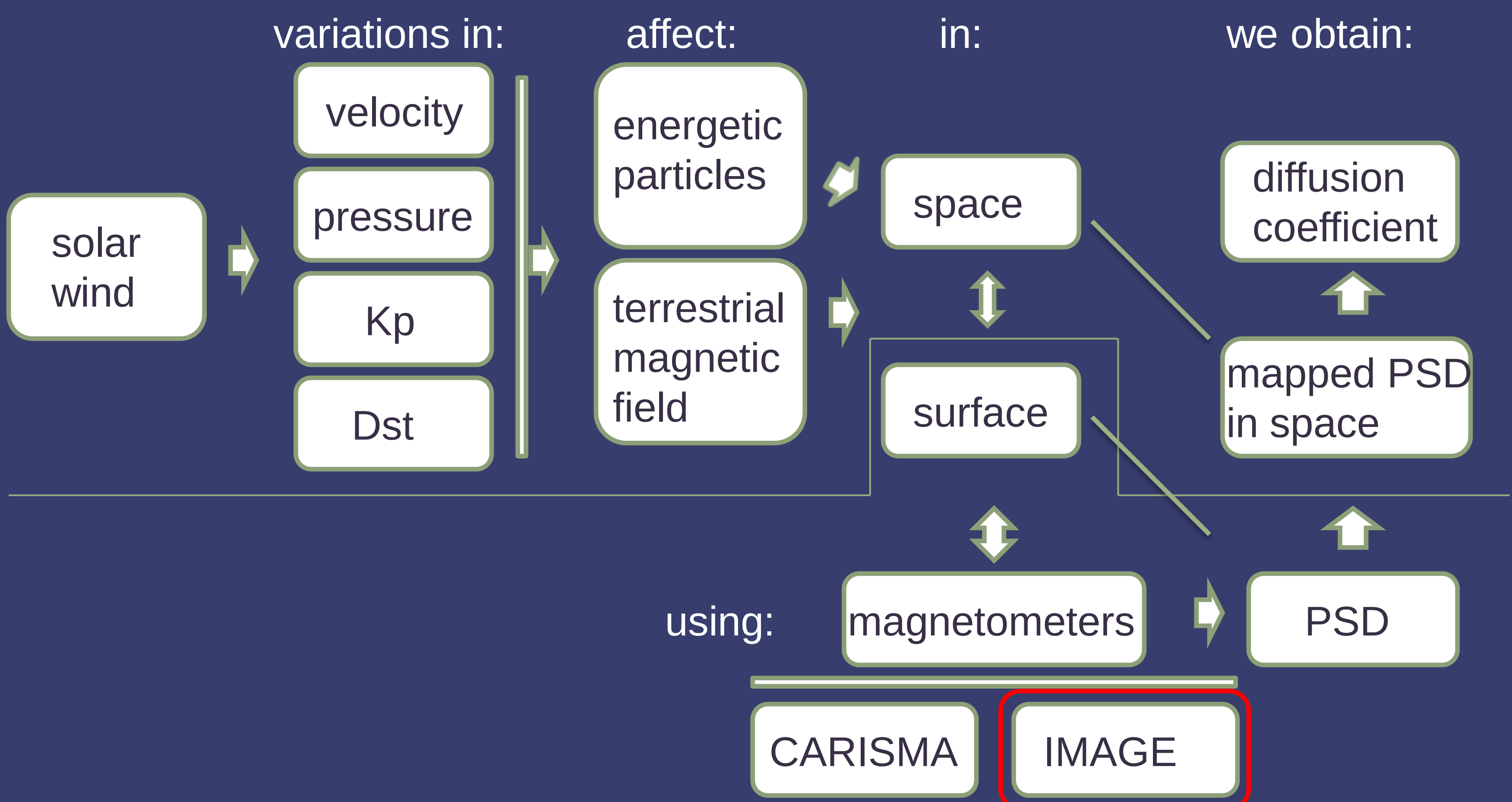

Objectives

1) Calculate the electric field diffusion coefficient using the methodology of Ozeke et al. (2012), using 11 years of European ground observations (IMAGE).

This step will offer a verification of the results of Ozeke et al. (2012), as well as an expansion of the statistical data, since European stations complement the North American ones. Also, a view of the waves at higher L-values.

2) Expand the research by binning the diffusion coefficient according to additional geomagnetic or solar wind parameters; binning by deciles.

With such a study we can ascertain which binning parameter gives the best resolution and, therefore, which parameter is most closely correlated with changes in the diffusion coefficient.

The model

Ozeke et al. 2012, JGR

Radial diffusion equation:
$$\frac{\partial f}{\partial t} = L^2 \frac{\partial}{\partial L}\left[\frac{D_{LL}}{L^2}\frac{\partial f}{\partial L}\right] - \frac{f}{\tau}$$

Diffusion coefficient:
$$D_{LL} = D_{LL}^E + D_{LL}^B$$

$$D_{LL}^E = \frac{1}{8B_E^2 R_E^2} L^6 \sum_m P_m^E(m\omega_d)$$

$$D_{LL}^B = \frac{M^2}{8q^2\gamma^2 B_E^2 R_E^4} L^4 \sum_m m^2 P_m^B(m\omega_d)$$

where: $M = \frac{p_\perp^2 L^3}{2m_e B_E}$ is the first adiabatic invariant.

$P_m^E(m\omega_d)$, $P_m^B(m\omega_d)$: PSD of the electric / magnetic field perturbations, for $\omega - m\omega_d = 0$

The IMAGE network

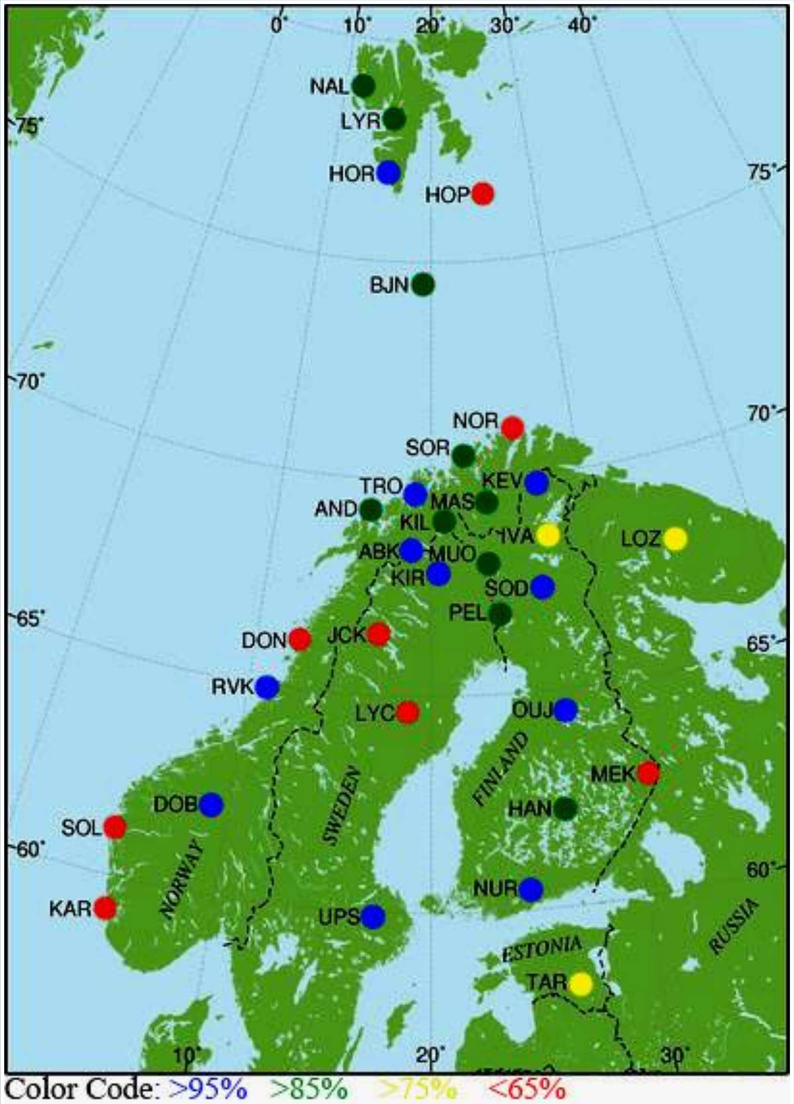

Station Locations (color coded according to data coverage for the years 2000 to 2010)

Code	Name	Geo.Lat. (°)	Geo.Lon. (°)	CGM Lat. (°)	CGM Lon. (°)	L-shell
HOR	Hornsund	77	15.6	74.13	109.59	13.6
TRO	Tromsø	69.66	18.94	66.64	102.9	6.46
KEV	Kevo	69.76	27.01	66.32	109.24	6.3
KIR	Kiruna	67.84	20.42	64.69	102.64	5.56
SOD	Sodankylä	67.37	26.63	63.92	107.26	5.26
RVK	Rørvik	64.94	10.98	62.23	93.31	4.68
OUJ	Oulujärvi	64.52	27.23	60.99	106.14	4.32
DOB	Dombås	62.07	9.11	59.29	90.2	3.89
NUR	Nurmijärvi	60.5	24.65	56.89	102.18	3.4
UPS	Uppsala	59.9	17.35	56.51	95.84	3.34

IMAGE data processing steps (TFA tool)

- Reading data (extended time interval to avoid edge effects)
- Checking for Data Gaps (set to NaN)
- Checking for FILL VALUES (set to NaN)
- Calculating Wavelet Power Spectral Density matrix at frequencies from 0.6 to 19.85 mHz (linearly spaced with a step of 0.25 mHz)
- Remove extended intervals
- Segment to hourly intervals
- Discard intervals with excessive NaNs
- Keep only daytime values

Balasis et al. 2012,
Annales Geophysicae

Balasis et al. 2013,
Earth, Planets and Space

PSDs on the ground

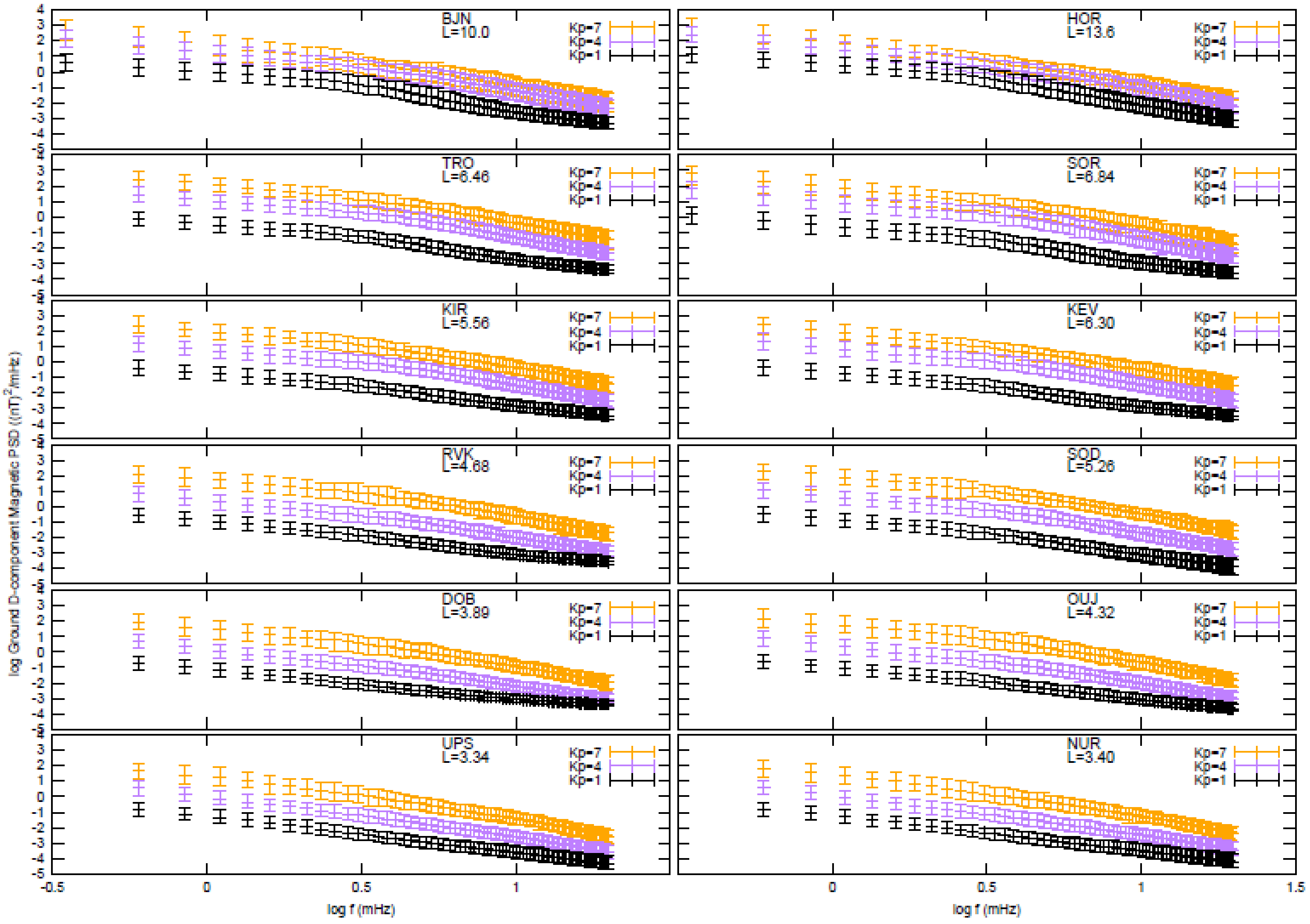

PSDs mapped to space

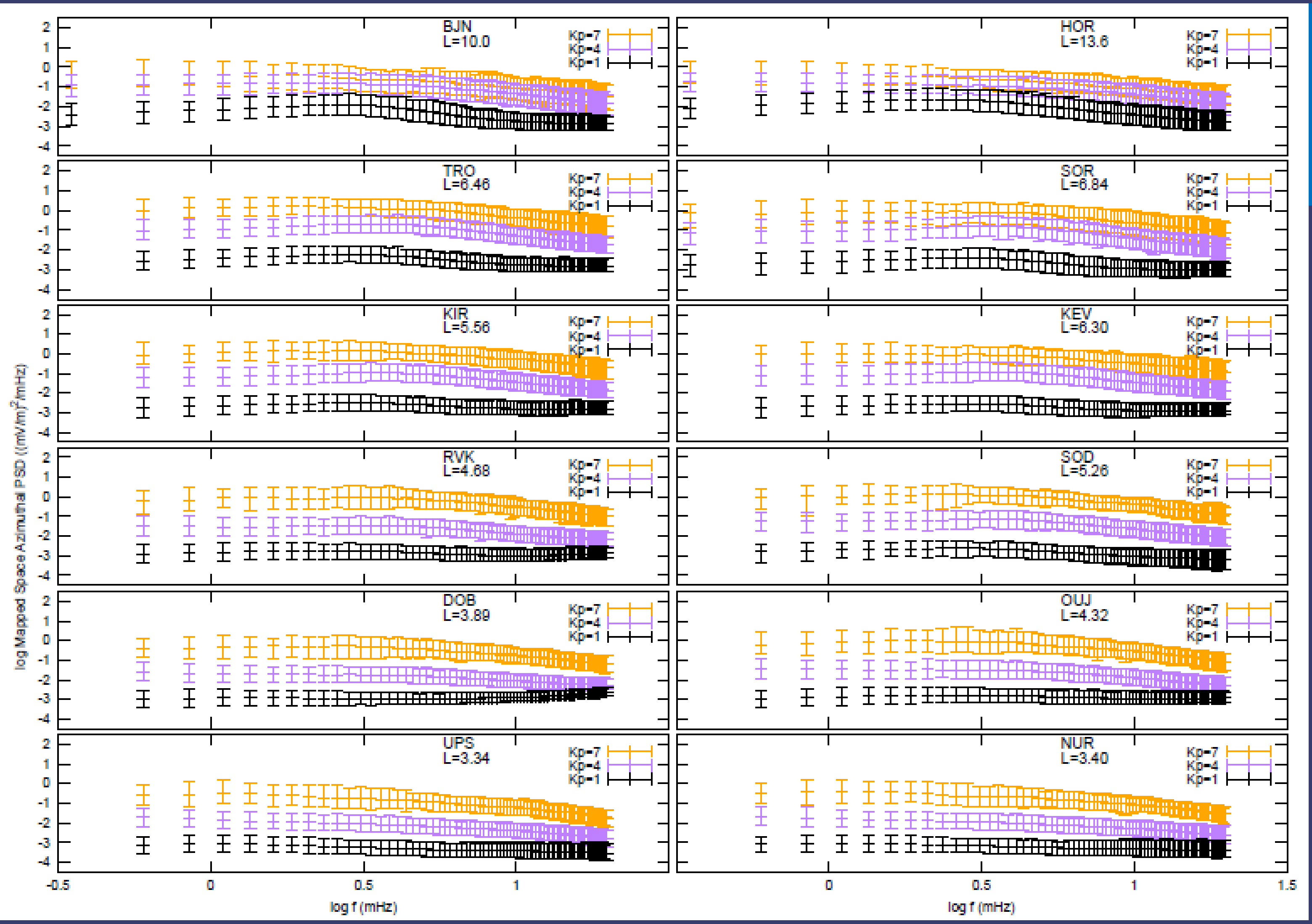

D^{E}_{LL}

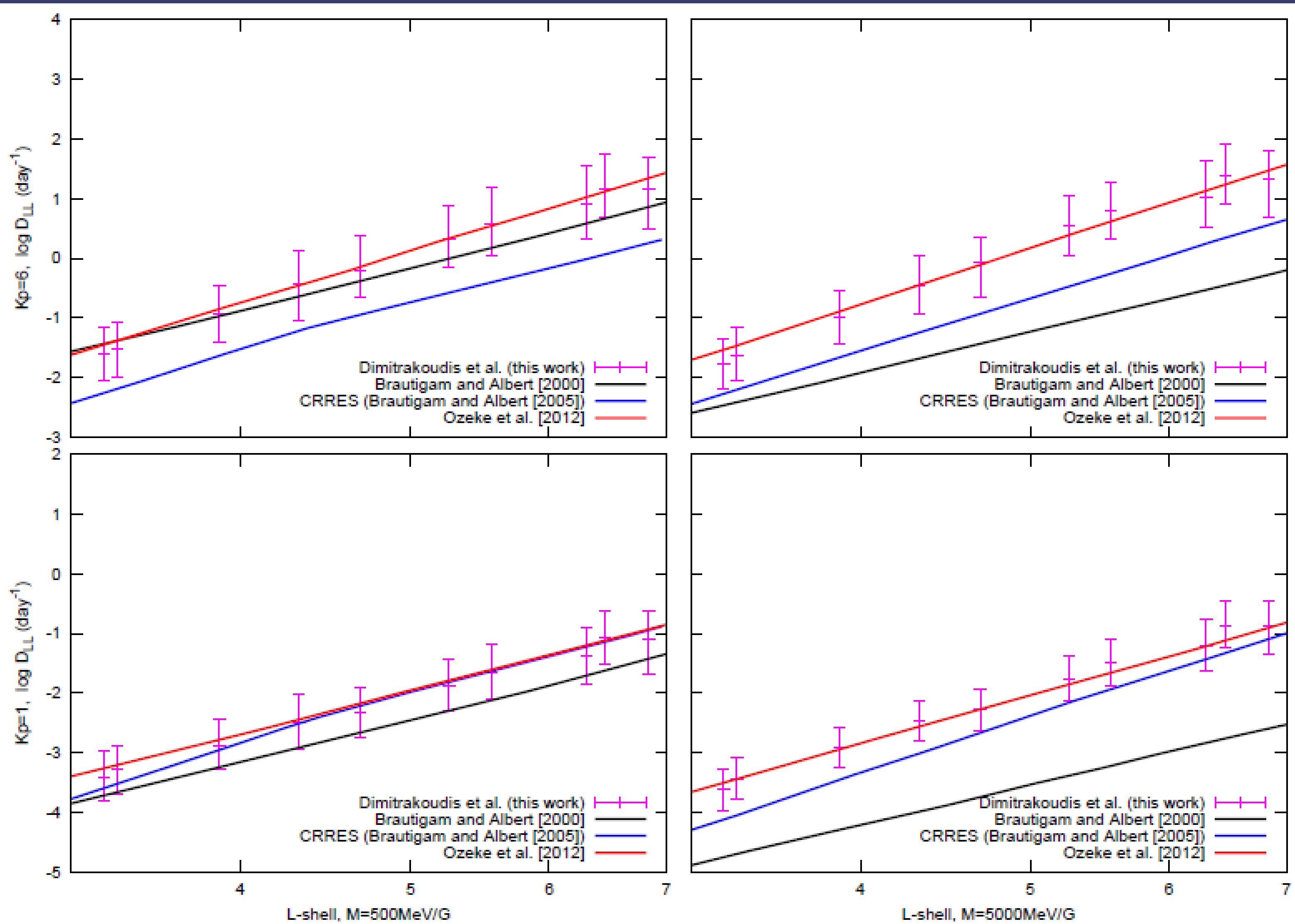

Kp=6, log D_LL (day^-1)
Kp=1, log D_LL (day^-1)
Dimitrakoudis et al. (this work)
Brautigam and Albert [2000]
CRRES (Brautigam and Albert [2005])
Ozeke et al. [2012]
Dimitrakoudis et al. (this work)
Brautigam and Albert [2000]
CRRES (Brautigam and Albert [2005])
Ozeke et al. [2012]
Dimitrakoudis et al. (this work)
Brautigam and Albert [2000]
CRRES (Brautigam and Albert [2005])
Ozeke et al. [2012]
Dimitrakoudis et al. (this work)
Brautigam and Albert [2000]
CRRES (Brautigam and Albert [2005])
Ozeke et al. [2012]
L-shell, M=500MeV/G
L-shell, M=5000MeV/G

Objectives

1) Calculate the electric field diffusion coefficient using the methodology of Ozeke et al. (2012), using 11 years of European ground observations (IMAGE).

This step will offer a verification of the results of Ozeke et al. (2012), as well as an expansion of the statistical data, since European stations complement the North American ones. Also, a view of the waves at higher L-values.

2) Expand the research by binning the diffusion coefficient according to additional geomagnetic or solar wind parameters; binning by deciles.

With such a study we can ascertain which binning parameter gives the best resolution and, therefore, which parameter is most closely correlated with changes in the diffusion coefficient.

Binning with other parameters

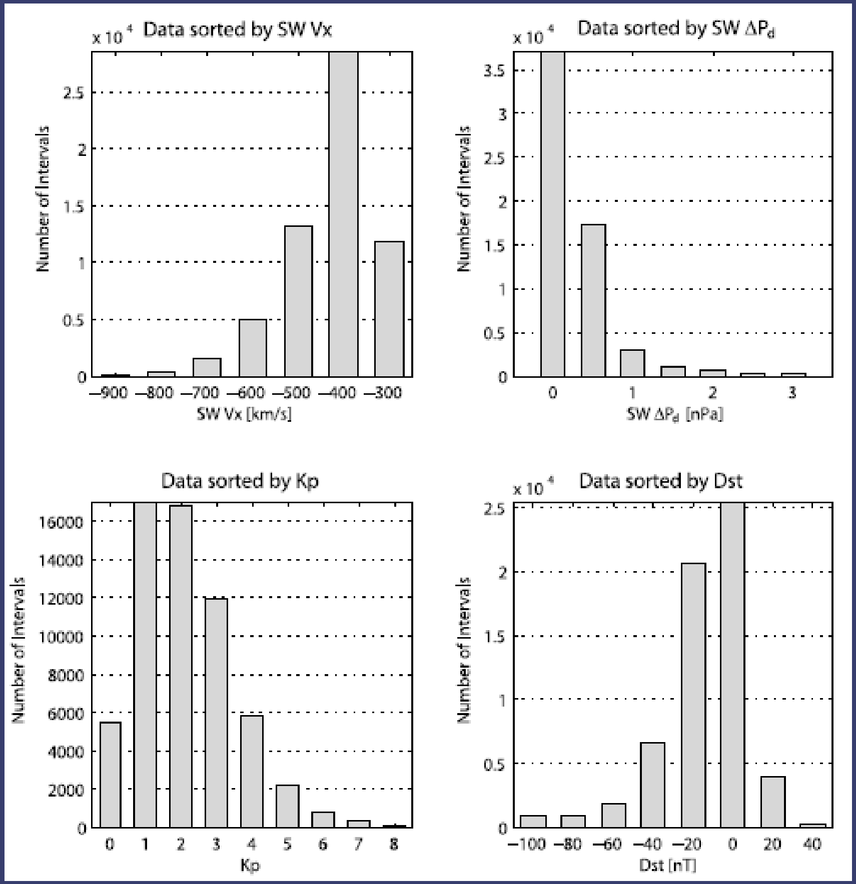

Huang et al. 2010

Binning with other parameters

Decile border	Kp	V_{sw}(km/s)	P_{dyn}(nPa)	Dst(nT)
0	0	233	0.03	67
1	0.3	320	0.81	6
2	0.7	346	1.01	1
3	1	369	1.19	-2
4	1.3	393	1.36	-6
5	1.7	418	1.57	-9
6	2	448	1.81	-13
7	2.7	485	2.14	-18
8	3	537	2.61	-25
9	3.7	607	3.54	-35
10	9	1189	79.05	-422

NUR
L=3.4

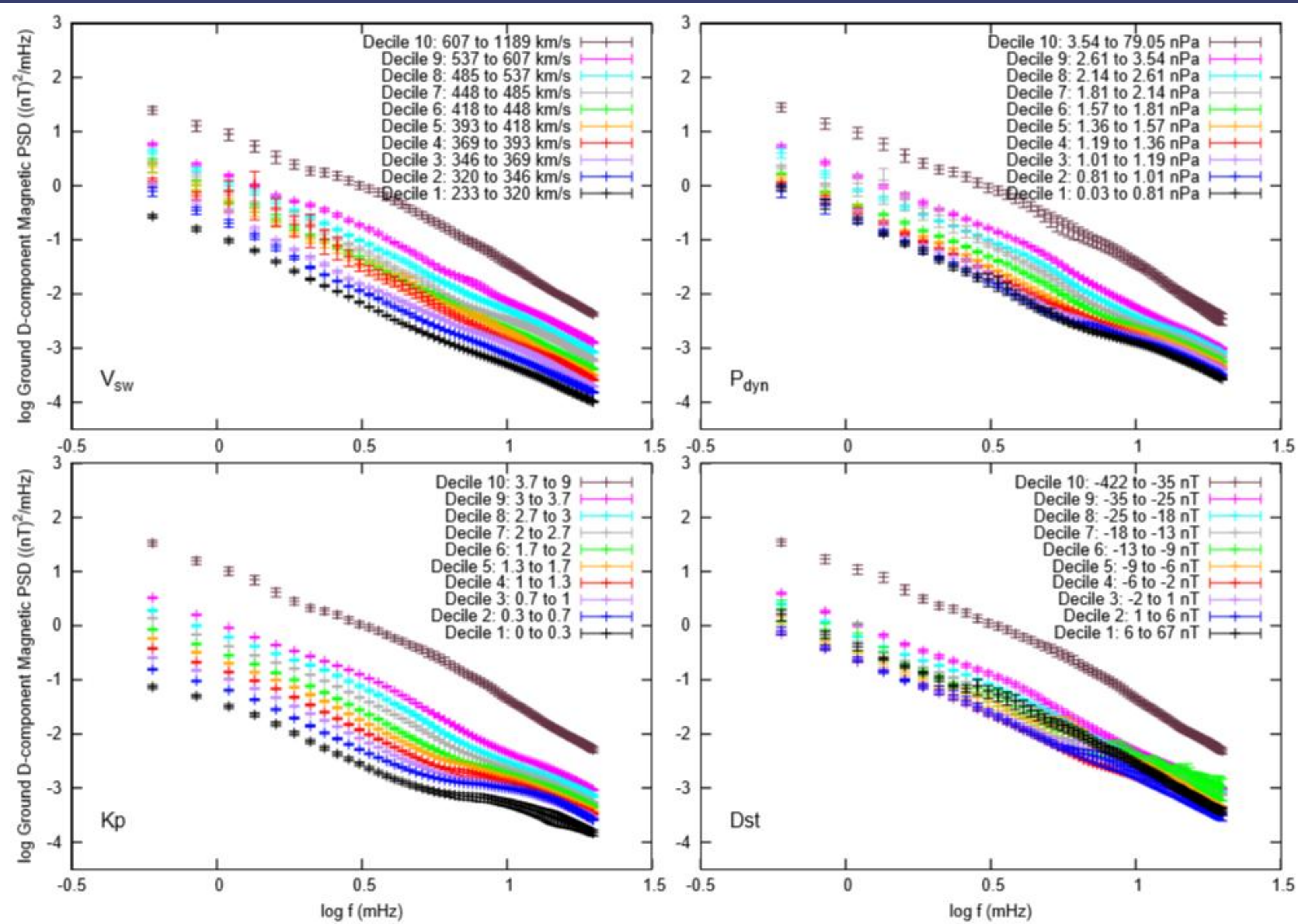

log Ground D-component Magnetic PSD ((nT)^2/mHz)
Decile 10: 607 to 1189 km/s
Decile 9: 537 to 607 km/s
Decile 8: 485 to 537 km/s
Decile 7: 448 to 485 km/s
Decile 6: 418 to 448 km/s
Decile 5: 393 to 418 km/s
Decile 4: 369 to 393 km/s
Decile 3: 346 to 369 km/s
Decile 2: 320 to 346 km/s
Decile 1: 233 to 320 km/s
V_{sw}
Decile 10: 3.54 to 79.05 nPa
Decile 9: 2.61 to 3.54 nPa
Decile 8: 2.14 to 2.61 nPa
Decile 7: 1.81 to 2.14 nPa
Decile 6: 1.57 to 1.81 nPa
Decile 5: 1.36 to 1.57 nPa
Decile 4: 1.19 to 1.36 nPa
Decile 3: 1.01 to 1.19 nPa
Decile 2: 0.81 to 1.01 nPa
Decile 1: 0.03 to 0.81 nPa
P_{dyn}
Decile 10: 3.7 to 9
Decile 9: 3 to 3.7
Decile 8: 2.7 to 3
Decile 7: 2 to 2.7
Decile 6: 1.7 to 2
Decile 5: 1.3 to 1.7
Decile 4: 1 to 1.3
Decile 3: 0.7 to 1
Decile 2: 0.3 to 0.7
Decile 1: 0 to 0.3
Kp
Decile 10: -422 to -35 nT
Decile 9: -35 to -25 nT
Decile 8: -25 to -18 nT
Decile 7: -18 to -13 nT
Decile 6: -13 to -9 nT
Decile 5: -9 to -6 nT
Decile 4: -6 to -2 nT
Decile 3: -2 to 1 nT
Decile 2: 1 to 6 nT
Decile 1: 6 to 67 nT
Dst
log f (mHz)

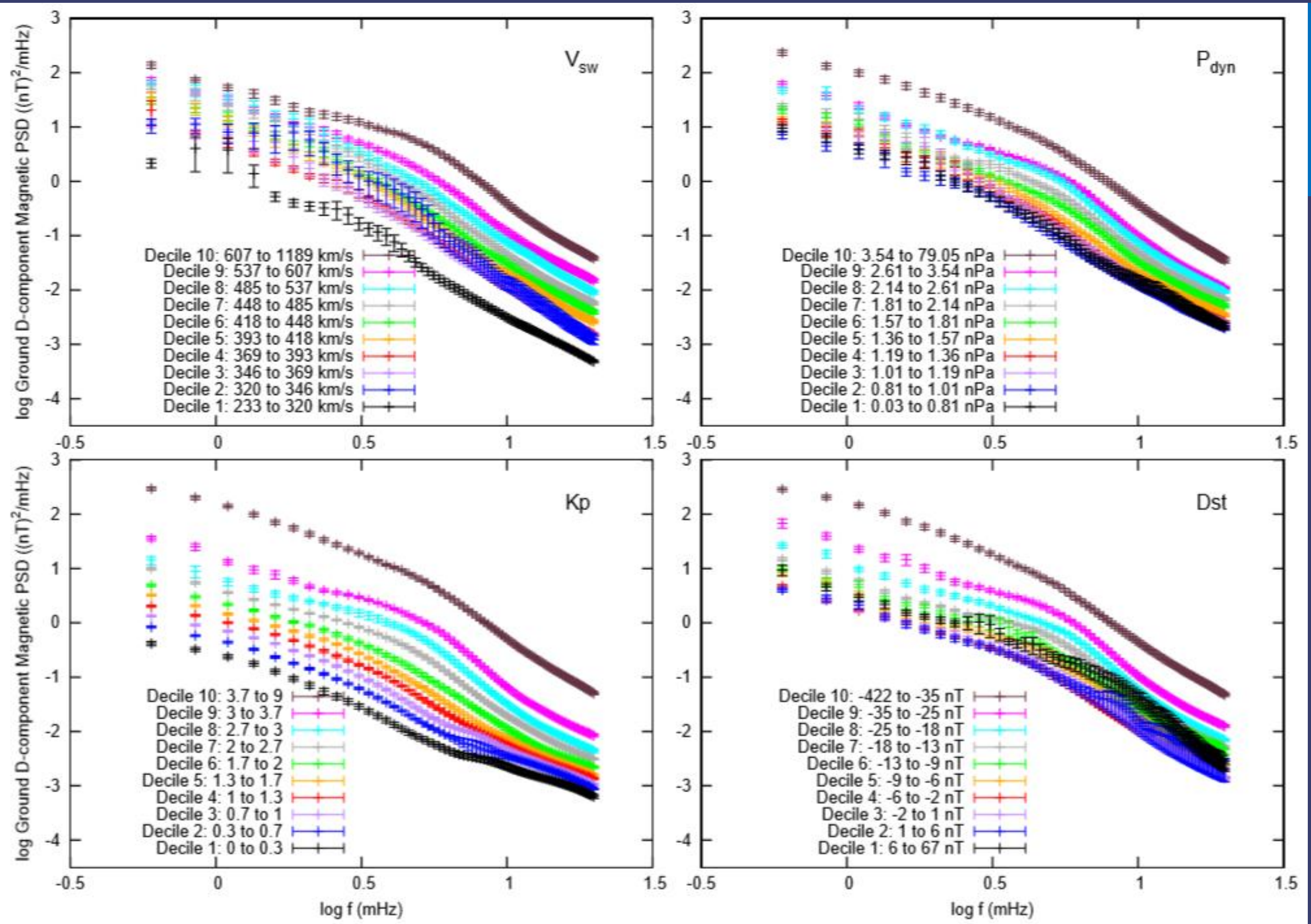

V_sw
P_dyn
Kp
Dst
log Ground D-component Magnetic PSD ((nT)^2/mHz)
log f (mHz)
Decile 10: 607 to 1189 km/s
Decile 9: 537 to 607 km/s
Decile 8: 485 to 537 km/s
Decile 7: 448 to 485 km/s
Decile 6: 418 to 448 km/s
Decile 5: 393 to 418 km/s
Decile 4: 369 to 393 km/s
Decile 3: 346 to 369 km/s
Decile 2: 320 to 346 km/s
Decile 1: 233 to 320 km/s
Decile 10: 3.54 to 79.05 nPa
Decile 9: 2.61 to 3.54 nPa
Decile 8: 2.14 to 2.61 nPa
Decile 7: 1.81 to 2.14 nPa
Decile 6: 1.57 to 1.81 nPa
Decile 5: 1.36 to 1.57 nPa
Decile 4: 1.19 to 1.36 nPa
Decile 3: 1.01 to 1.19 nPa
Decile 2: 0.81 to 1.01 nPa
Decile 1: 0.03 to 0.81 nPa
Decile 10: 3.7 to 9
Decile 9: 3 to 3.7
Decile 8: 2.7 to 3
Decile 7: 2 to 2.7
Decile 6: 1.7 to 2
Decile 5: 1.3 to 1.7
Decile 4: 1 to 1.3
Decile 3: 0.7 to 1
Decile 2: 0.3 to 0.7
Decile 1: 0 to 0.3
Decile 10: -422 to -35 nT
Decile 9: -35 to -25 nT
Decile 8: -25 to -18 nT
Decile 7: -18 to -13 nT
Decile 6: -13 to -9 nT
Decile 5: -9 to -6 nT
Decile 4: -6 to -2 nT
Decile 3: -2 to 1 nT
Decile 2: 1 to 6 nT
Decile 1: 6 to 67 nT

TRO
L=6.46

Power comparison

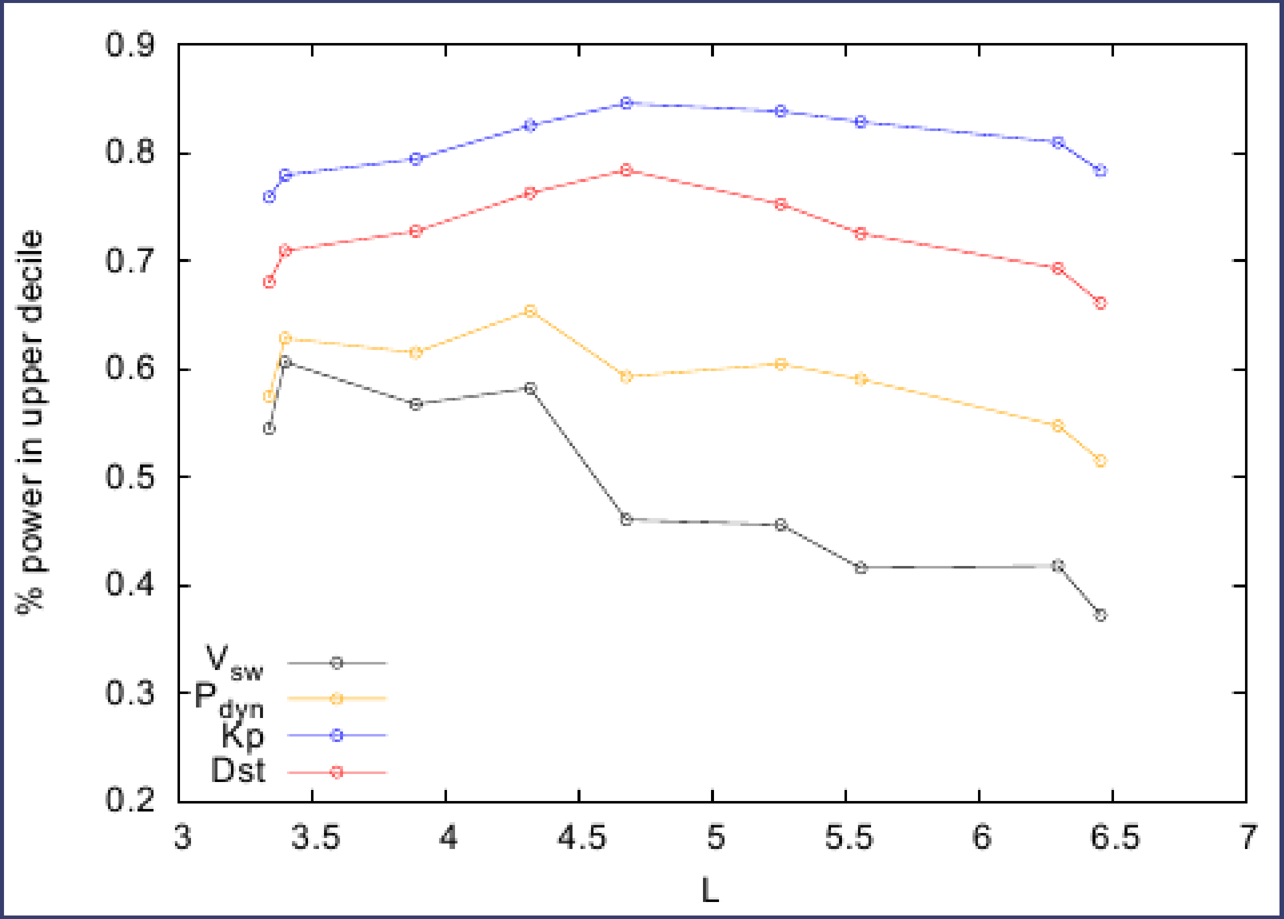

TRO
L=6.46
percentiles

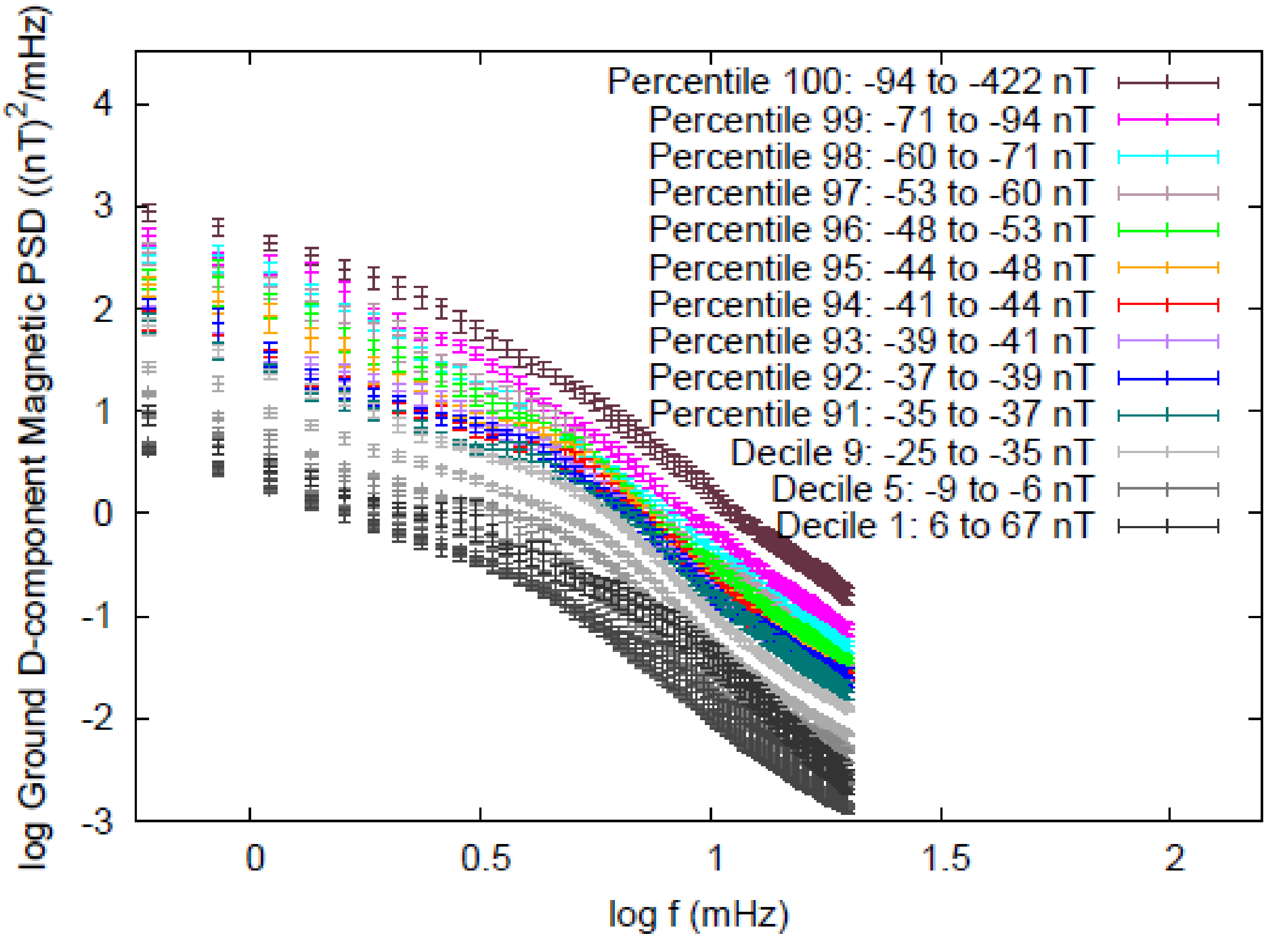

hours per decile combo

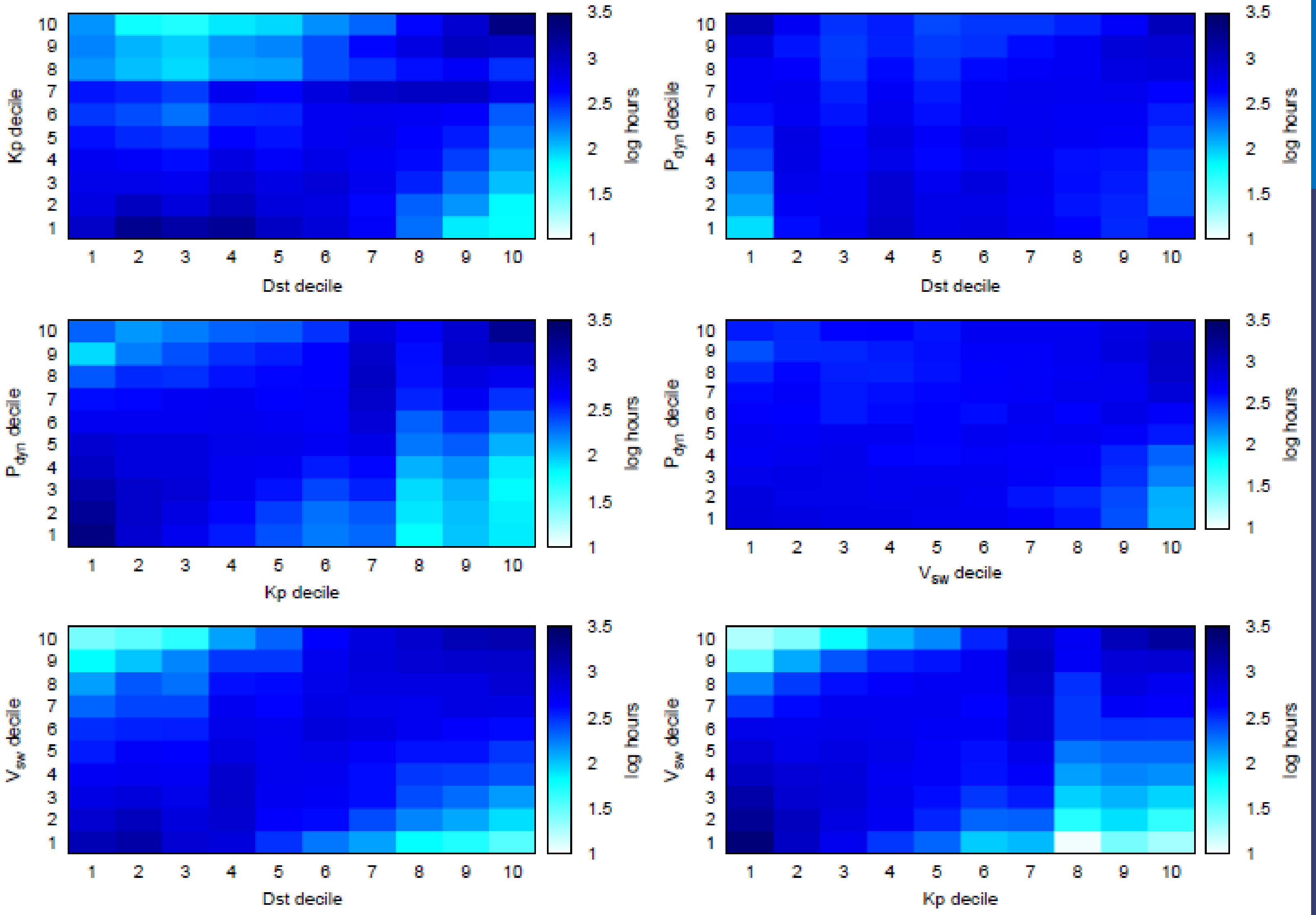

UPS
L=3.34

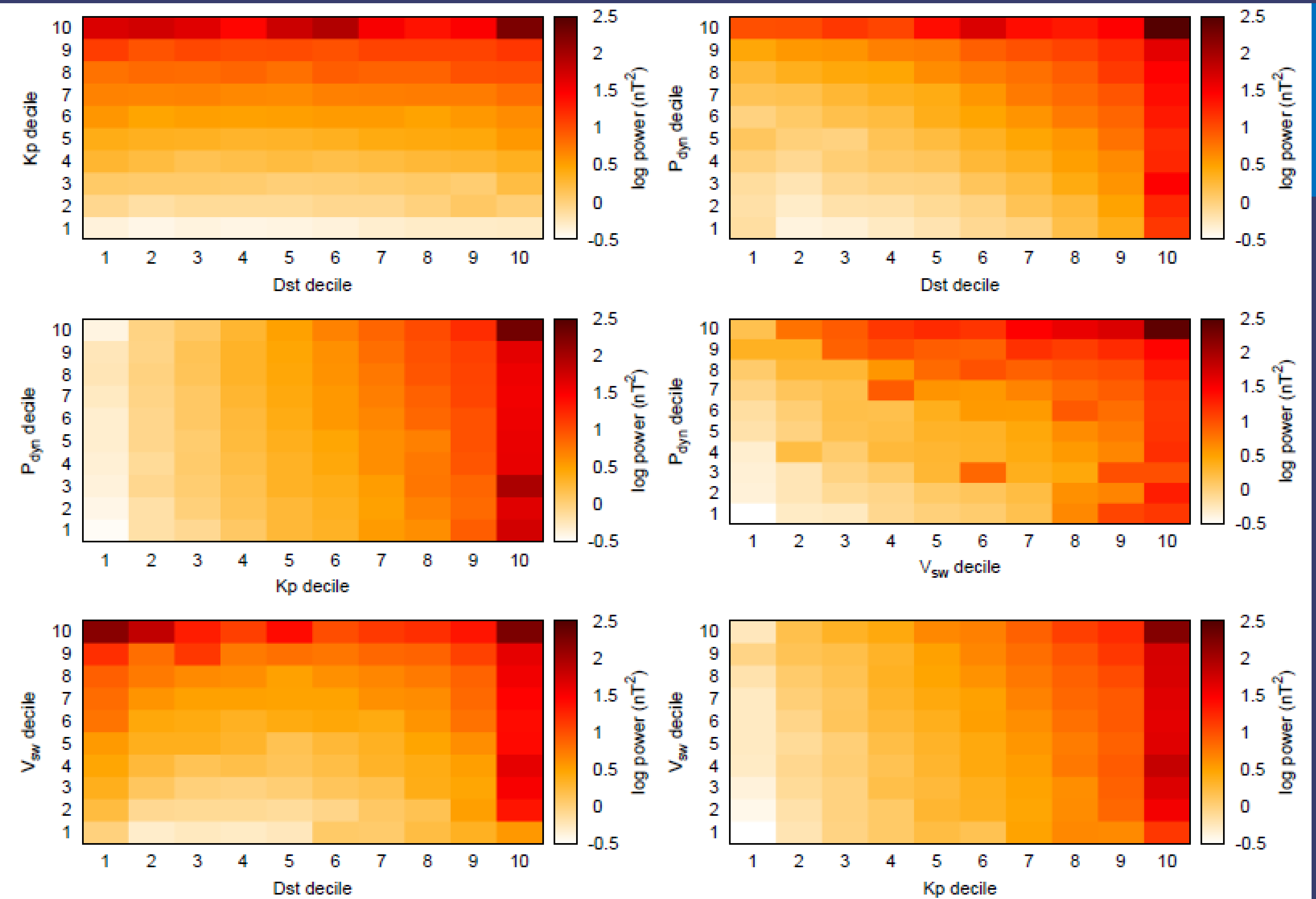

Kp decile
Dst decile
P_{dyn} decile
Kp decile
V_{sw} decile
log power (nT^2)
1 2 3 4 5 6 7 8 9 10
-0.5 0 0.5 1 1.5 2 2.5

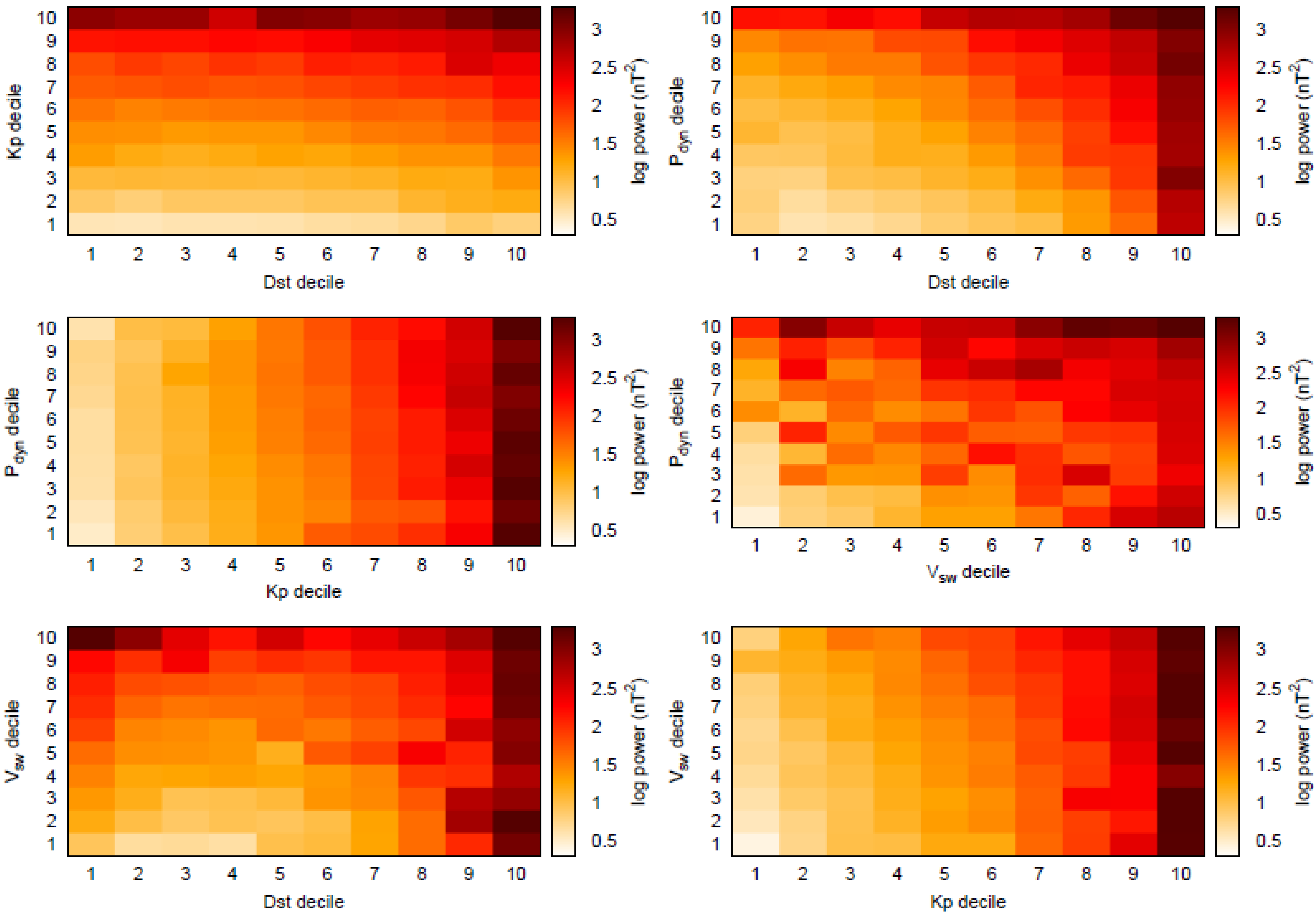
Kp decile
Dst decile
log power (nT^2)
P_{dyn} decile
Dst decile
log power (nT^2)
P_{dyn} decile
Kp decile
log power (nT^2)
P_{dyn} decile
V_{sw} decile
log power (nT^2)
V_{sw} decile
Dst decile
log power (nT^2)
V_{sw} decile
Kp decile
log power (nT^2)

TRO
L=6.46

Summary

1) Our results corroborate the Ozeke 2012/2014 results, using:

i) Temporally and longitudinally different data (IMAGE instead of CARISMA)
ii) Different data analysis (wavelets instead of FFT)

2) After binning by deciles for various parameters, we observe:

i) Better resolution when binning by Kp
ii) Up to half of the variability is contained in the upper decile
iii) ULF power well ordered even within the top decile
iv) Upper decile power ratio peaks at around L ~ 4.3 to 4.7
v) Dst is better determinant of top ULF power

Bonus slides: Higher L-shells

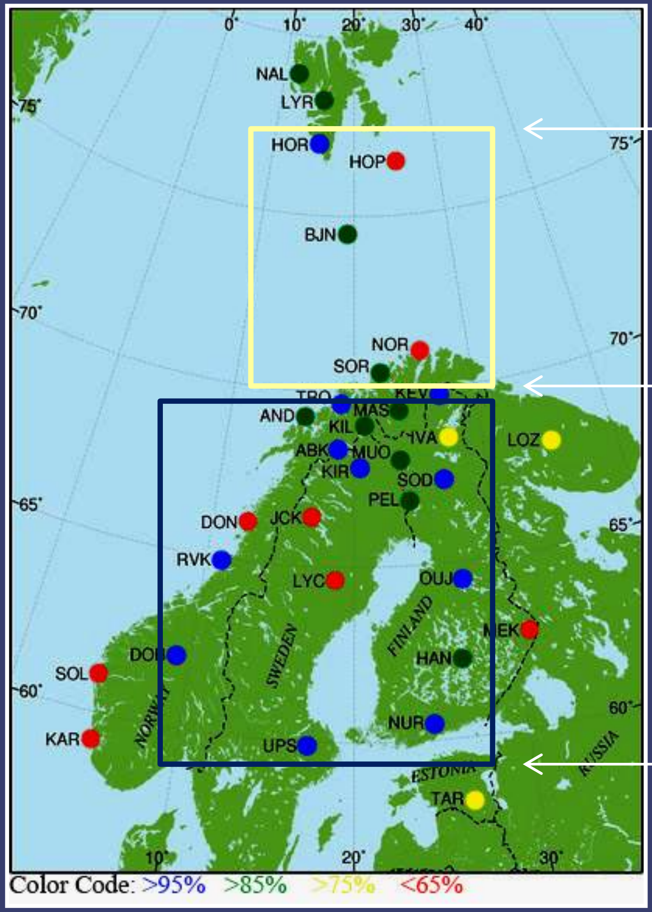

L = 13

L = 6.46

L = 3.34

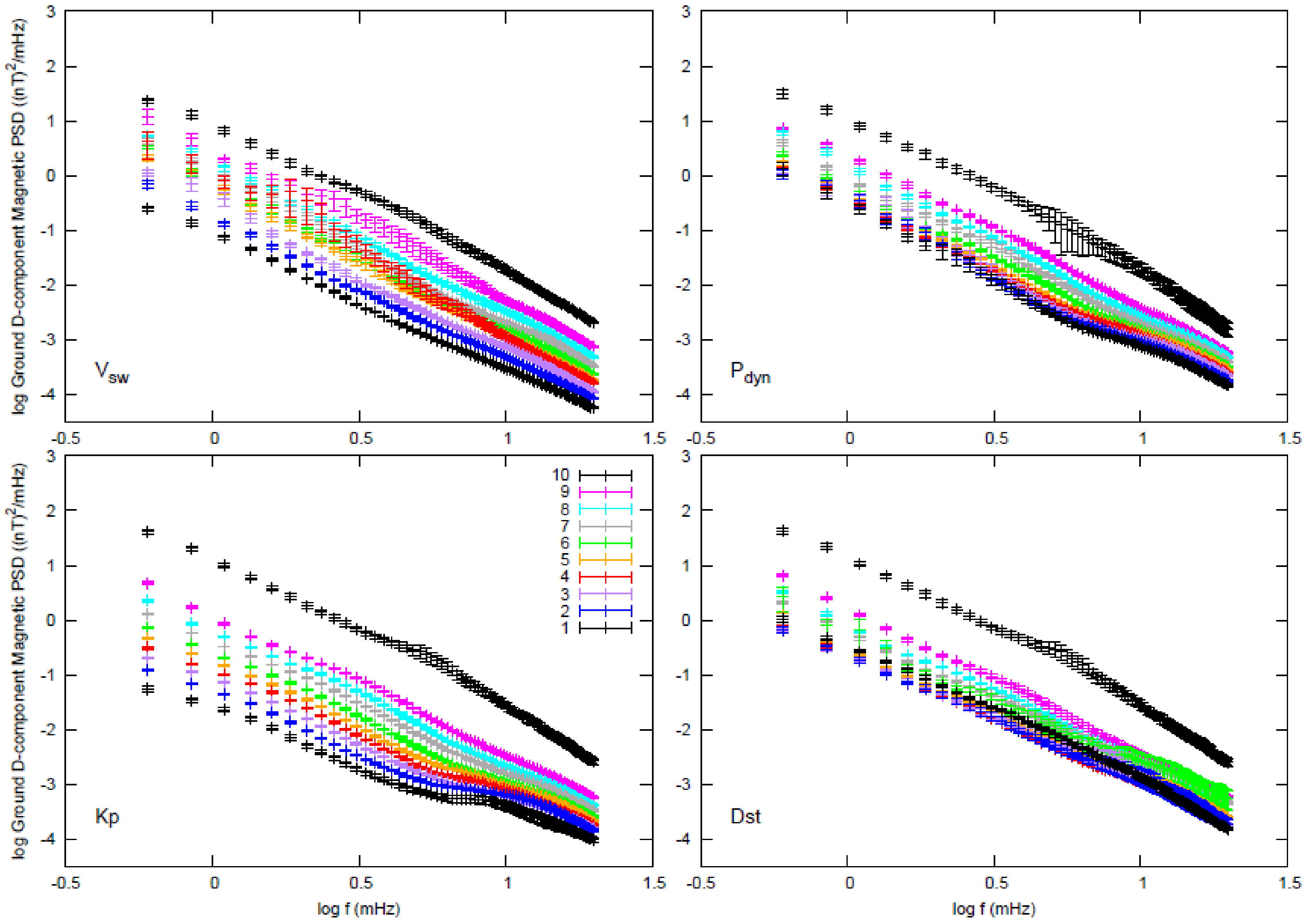

Vsw
Pdyn
Kp
Dst
log Ground D-component Magnetic PSD ((nT)^2/mHz)
log f (mHz)
10
9
8
7
6
5
4
3
2
1

UPS
L=3.34

SOR
L=6.84

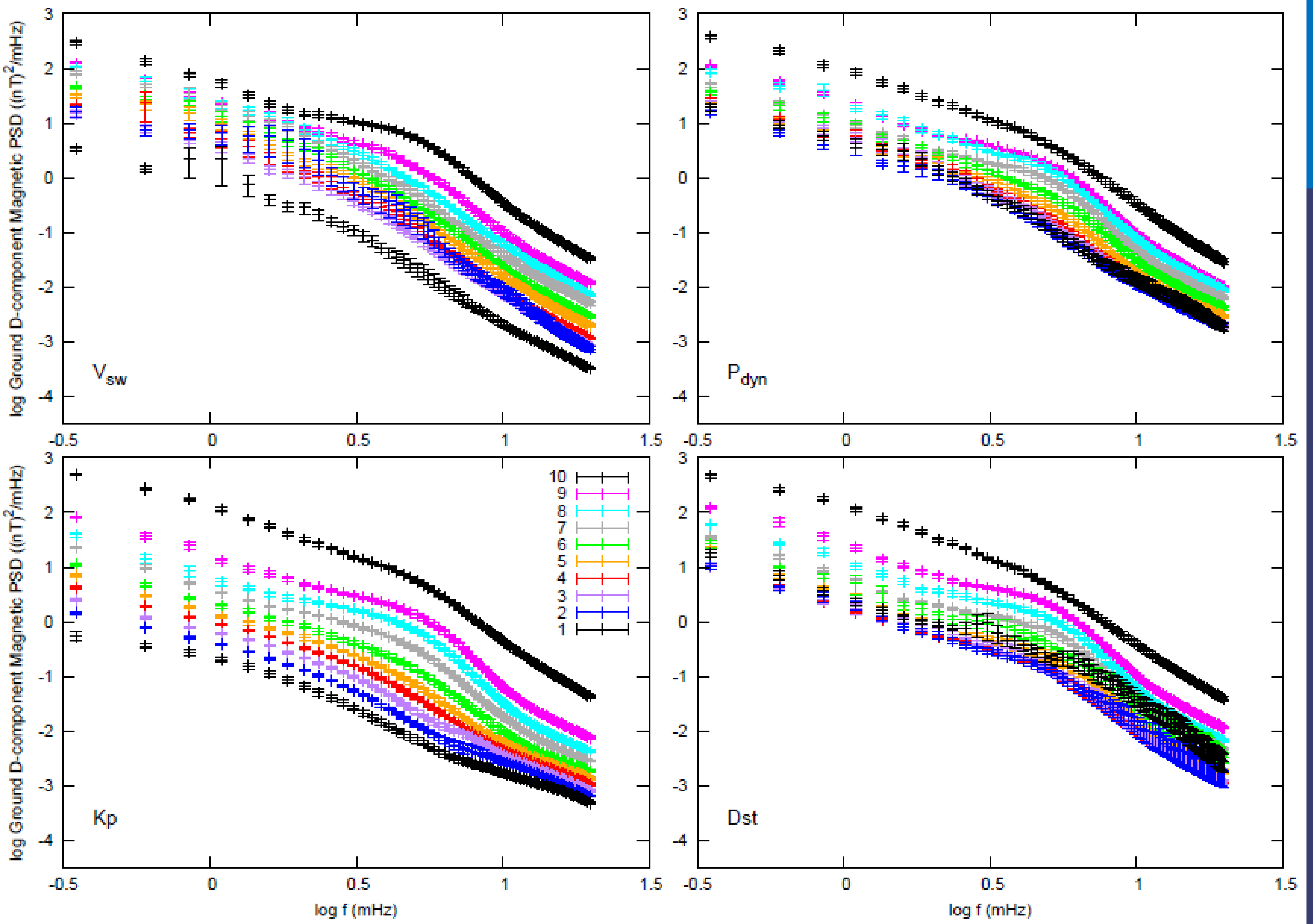
log Ground D-component Magnetic PSD ((nT)^2/mHz)
log f (mHz)
V_{sw}
P_{dyn}
Kp
Dst
10
9
8
7
6
5
4
3
2
1

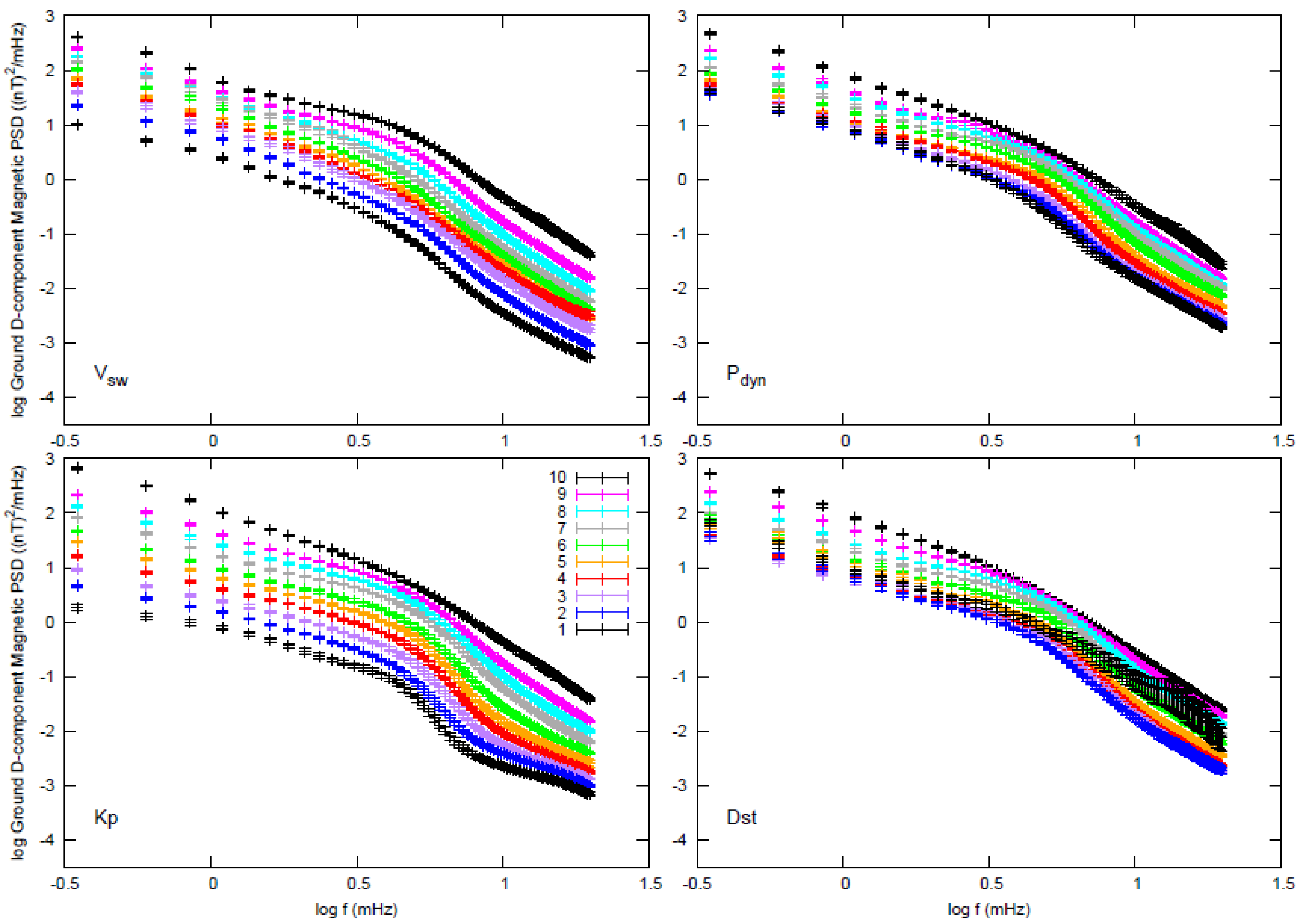
log Ground D-component Magnetic PSD ((nT)²/mHz)
log f (mHz)
Vsw
Pdyn
Kp
Dst
10
9
8
7
6
5
4
3
2
1

BJN
L=10

HOR
L=13.6

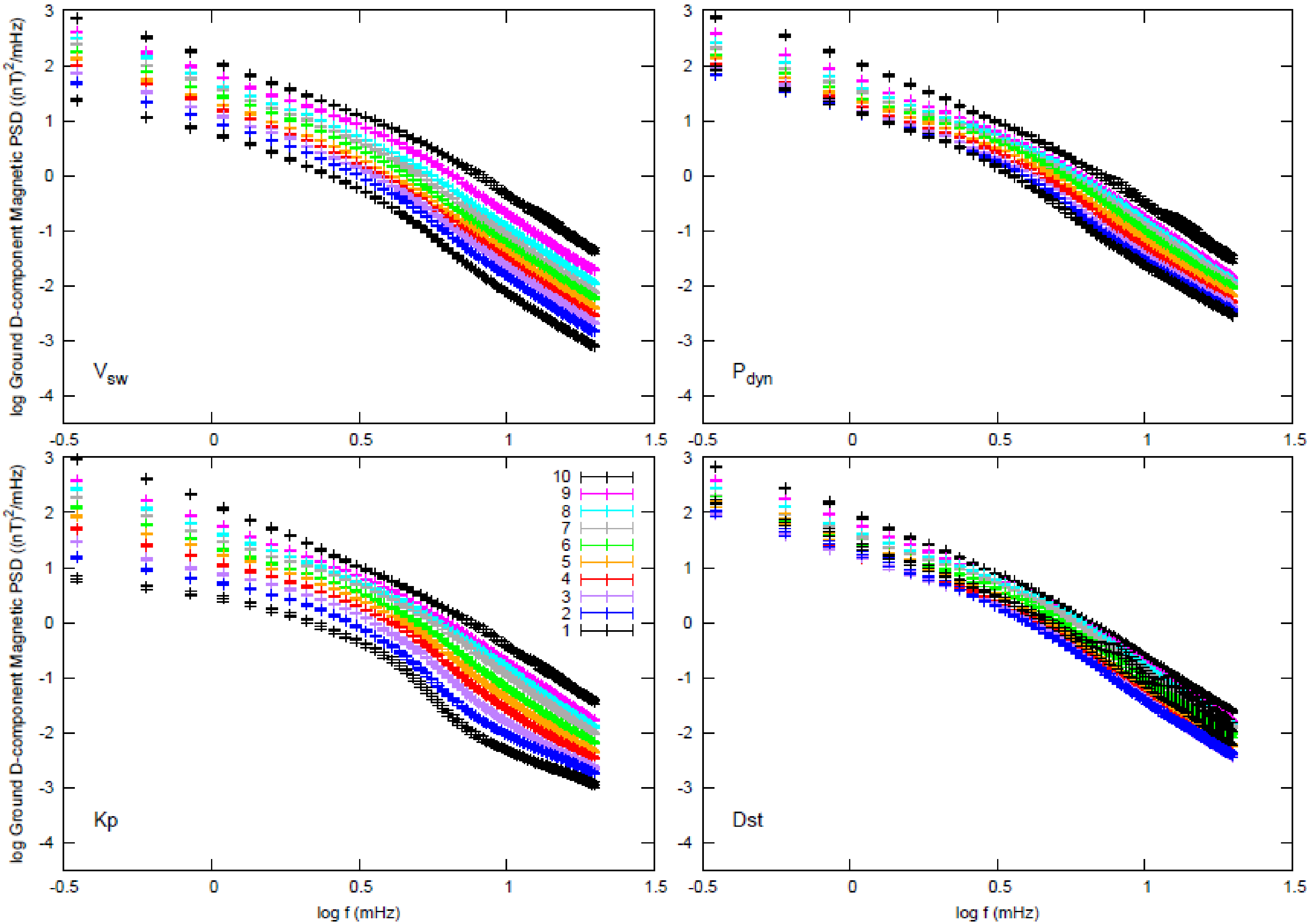

log Ground D-component Magnetic PSD ((nT)^2/mHz)
V_{sw}
P_{dyn}
Kp
Dst
10
9
8
7
6
5
4
3
2
1
log f (mHz)

% power in upper decile

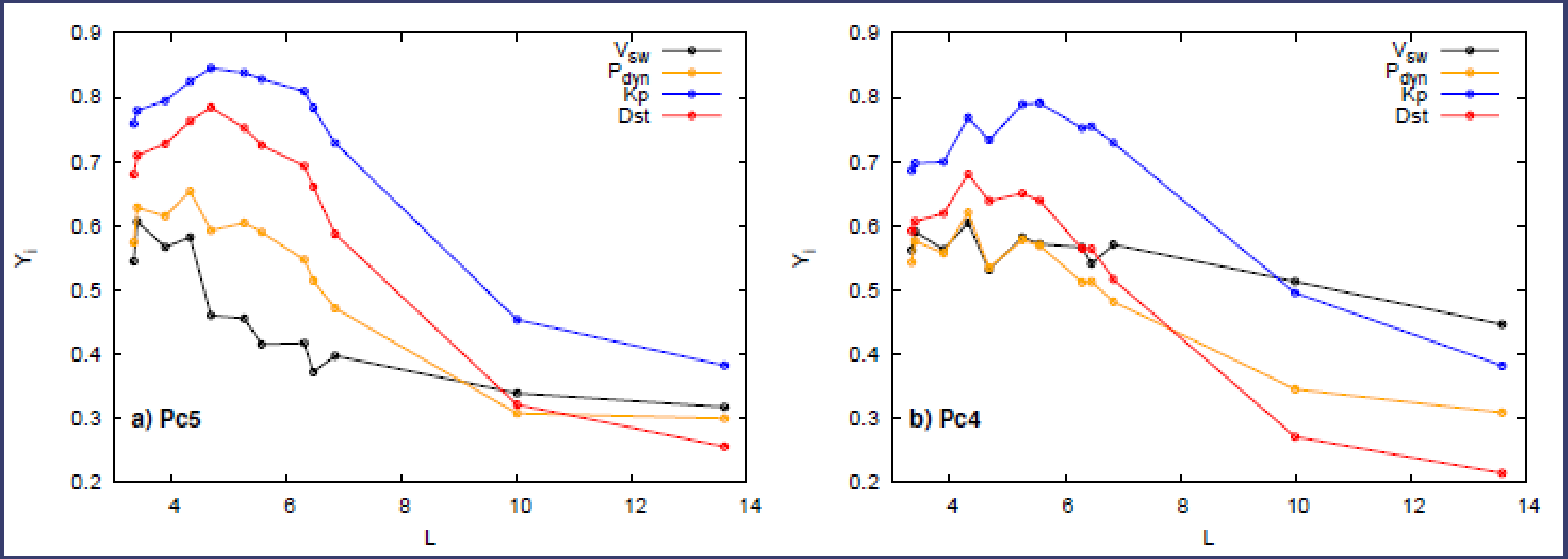

Thank you!

This work has received funding from the European Union's Seventh Framework Programme (**FP7**-SPACE-2011-1) under grant agreement n. 284520 for the **MAARBLE** (Monitoring, Analyzing and Assessing Radiation Belt Loss and Energization) collaborative research project. We acknowledge support from the "**Hellenic National Space Weather Research Network**" co-financed by the European Union (European Social Fund **ESF**) and Greek national funds through the Operational Program "Education and Lifelong Learning" of the National Strategic Reference Framework (NSRF) Research Funding Program "**Thales**. Investing in knowledge society through the European Social Fund".